Eur. Phys. J. B **55**, 419–427 (2007)
DOI: 10.1140/epjb/e2007-00080-0

THE EUROPEAN PHYSICAL JOURNAL B

Shot noise in a quantum dot coupled to carbon nanotube terminals applied with a microwave field

H.-K. Zhao[1,2,a] and Q. Chen[2]

[1] CCAST (World Laboratory), P.O. Box 8730, Beijing 100080, P.R. China
[2] Department of Physics, Beijing Institute of Technology, Beijing 100081, P.R. China

Received 13 October 2006 / Received in final form 5 February 2007
Published online 22 March 2007

Abstract. We have investigated the spectral density of shot noise for the system of a quantum dot (QD) coupled to two single-wall carbon nanotube terminals irradiated with a microwave field on the QD. The terminal features are involved in the shot noise through modifying the self-energy of QD. The contributions of carbon nanotube terminals to the shot noise exhibit obvious behaviors. The novel side peaks are associated with the photon absorption and emission procedure accompanying the suppression of shot noise. The shot noise in balanced absorption belongs to sub-Poissonian, and it is symmetric with respect to the gate voltage. The differential shot noise displays intimate relation with the nature of carbon nanotubes and the applied microwave field. It exhibits asymmetric behavior for the unbalanced absorption case versus gate voltage. The Fano factor of the system exhibits the deviation of shot noise from the Schottky formula, and the structures of terminals obviously contribute to it. The super-Poissonian and sub-Poissonian shot noise can be achieved in the unbalanced absorption in different regime of source-drain bias.

PACS. 85.35.-p Nanoelectronic devices – 73.23.-b Electronic transport in mesoscopic systems – 73.63.Fg Nanotubes – 73.21.La Quantum dots

1 Introduction

Shot noise is the phenomenon related to nonequilibrium correlation behaviors for the discrete charged particles moving in definite direction to form measurable current $\langle I \rangle$. The thermal noise, on the other hand, is the equilibrium effect of fluctuations in the occupation number of electron, which can be obtained from the measurement of conductance. However, the information of shot noise can not be derived from the measurement of conductance. Instead, we have to investigate nonequilibrium state of a system [1,2]. Quantum effects in a mesoscopic system make important contributions to shot noise. Classically, the well-known Schottky's formula $S_P = 2e\langle I \rangle$ is the shot noise corresponding to uncorrelated transporting particles with the Poissonian distribution [3], which is referred to as the Poisson value of shot noise. The quantum behaviors of shot noise mainly arise from the coherent mesoscopic transport, the suppression of shot noise due to Pauli exclusion principle, and the Fermi distribution of electrons. In general, the current operator can be described by the creation and annihilation operators of electrons, and the interchange of operators induces novel terms, which contribute to the noise in quantum mechanics point of view. The shot noise is composed of four correlated nonequilibrium particle operators, which induce novel behaviors in the current correlation [4,5]. The shot noise can be obtained as the temperature approaches zero, which is the excess noise. Obtaining shot noise of deviation from Schottky's form is found to be interesting. The Pauli suppression of shot noise has been demonstrated experimentally by several groups [6–9]. The shot noise suppression in one-dimensional hopping model [10], the suppression by Fermi and Coulomb interaction [11] have been discussed. The enhanced shot noise was derived theoretically by considering the diode biased resonant tunneling system in the negative differential resistance regions [12]. The enhancement of shot noise was observed in the case of resonant tunneling via localized states [13].

The single-wall carbon nanotubes (CNs) are investigated intensively due to their interesting properties in electronics [14,15]. The specific behaviors on electron transport in these materials arise further systematically studies on the potential application in manipulation of quantum devices, such as the diode [16], heterojunction [17], and field effect transistor [18]. The CN systems coupling to different materials contain unexpected feature which could be used in the future logic circuit constructions [19]. The basic problems on mesoscopic transport through the CN based devices present profound investigation phenomena, and consequently We have very active

[a] e-mail: zhaohonk@yahoo.com

research frontier both in theoretical and experimental aspects [20–26]. A nano-device is often applied with a microwave field (MWF) through its gate or source-drain terminals. The time-dependent field induces nonlinear photon-assisted tunneling, and the time-reversal symmetry is broken [27–29]. The information of external field is transferred to the tunneling current and differential conductance. Recently, we have made series investigations on mesoscopic transport through the systems composed of carbon nanotubes under the perturbation of external MWFs, such as the system with a quantum dot coupled to two carbon nanotubes, and the system with a toroidal carbon nanotube coupled to two normal metal terminals. Novel characteristics are revealed to be associated with the photon-assisted tunneling [30], the periodical oscillation in the magnetic flux [31], and the spin-current resonant structures [32].

In this paper, we investigate the photon-assisted shot noise spectral density in the mesoscopic system with a quantum-dot (QD) coupled to single-wall carbon nanotube leads (CN-QD-CN). The central QD is applied with a time-dependent field through its gate. The CN terminals act as quantum wires which open multi-channels for electron to transport through. Since a CN lead has its own feature associated with the concrete CN structure, the density of state (DOS) plays an important role in the mesoscopic transport. The photon-assisted shot noise has been investigated by Pedersen and Büttiker [33] using the scattering theory for a contact system, and by Sun et al. [34] through employing the equation of motion method to study the single-level QD system. Since our system is different from theirs, the corresponding formulas are also derived to contain novel physical properties associated with concrete mesoscopic structure. We employ the equation of motion method to find electron operators, and then obtain the current operator from the continuity equation. The nonequilibrium Green's functions are involved in the current operator, and the shot noise spectral density is derived through Fourier transformation of current correlations. We arrange the formula derivation in Section 2, and the numerical calculations in Section 3. Brief discussion is presented in the last section.

2 Model and formalism

We consider the circumstance that a QD is coupled to two single-wall carbon nanotubes (CN-QD-CN). An external MWF irradiates to the QD through its gate, which is equivalent to the case that a time-dependent electric field is applied to the central QD through its gate. This induces an electric dipole potential to modify the energy spectrum of central QD as $E_{\ell\sigma}(t) = \tilde{E}_{\ell\sigma} + eV_d \cos\omega t - eV_g$, where $\tilde{E}_{\ell\sigma}$ is the isolated energy of QD in the absence of external field, and V_g is the gate voltage. We consider the relatively large QD which can be expressed by a noninteracting electron system approximately. The CN leads are described by the tight-binding Hamiltonian. The terminals are taken in equilibrium states which can be expressed by the grand canonical ensembles. The electronic properties can be determined by the total Hamiltonian which is the summation of sub-Hamiltonians and tunneling interaction terms

$$H = \sum_{\delta\gamma k\sigma} \varepsilon_{\delta\gamma,k\sigma} c^{\dagger}_{\delta\gamma,k\sigma} c_{\delta\gamma,k\sigma} + \sum_{\ell\sigma} E_{\ell\sigma}(t) d^{\dagger}_{\ell\sigma} d_{\ell\sigma} + \sum_{\delta\gamma k\ell\sigma} [R_{\gamma} c^{\dagger}_{\delta\gamma,k\sigma} d_{\ell\sigma} + H.c.], \quad (1)$$

where $c^{\dagger}_{\delta\gamma,k\sigma}(c_{\delta\gamma,k\sigma})$, and $d^{\dagger}_{\ell\sigma}(d_{\ell\sigma})$ are the creation (annihilation) operators of electron in two leads and central QD, respectively, with $\gamma \in \{L, R\}$. R_{γ} is the interaction strength of electrons between the γth lead and the central QD. We take the chemical potential of the right lead as the reference of energy measurement. The spin σ has the values as $+1$ and -1 corresponding to the notations $\uparrow$ and $\downarrow$, respectively, in the subscripts of equations. The energy of a CN lead $\varepsilon_{\delta\gamma,k\sigma}$ is intimately associated with the structure of concrete CN. We present the energy of armchair CN in the tight-binding approximation here as an example [15]

$$\varepsilon_{\delta\gamma,k\sigma} = \delta\gamma_0 \left\{ 1 + 4\cos\left(\frac{ak_y}{2}\right)\cos\left(\frac{\sqrt{3}ak_x}{2}\right) + 4\cos^2\left(\frac{ak_y}{2}\right) \right\}^{\frac{1}{2}}, \quad (2)$$

where $\sqrt{3}ak_x/2 = \pi q/n$, $q = 1, 2, \ldots, 2n$, $\delta = \pm$, and $\gamma_0 = 3.033$ eV. The energy in the transversal direction is quantized, while in the longitudinal direction it is not restricted. To proceed conveniently, we make the gauge transformation over the system by letting $\Psi(t) = \hat{U}(t)\tilde{\Psi}(t)$ in the Schrödinger equation, where the unitary operator $\hat{U}(t)$ is defined by $\hat{U}(t) = \exp(-i\lambda \sum_{\ell\sigma} d^{\dagger}_{\ell\sigma} d_{\ell\sigma} \sin\omega t)$, with $\lambda = eV_d/\hbar\omega$. The Hamiltonian of the system undergoes the gauge transformation $\tilde{H} = \hat{U}^{-1}(t) H \hat{U}(t)$. The transformed Hamiltonian is obtained by letting $E_{\ell\sigma} \to \tilde{E}_{\ell\sigma} - eV_g$, and the interaction strengths $R_{\gamma} \to \tilde{R}_{\gamma}(t) = R_{\gamma} \exp(-i\lambda \sin\omega t)$ in equation (1).

The shot noise spectral density $S_{\gamma\gamma'}(\Omega)$ is determined by the Fourier transformation of the current correlation

$$\Pi_{\gamma\gamma'}(t, t') = \langle \delta\hat{I}_{\gamma}(t) \delta\hat{I}_{\gamma'}(t') \rangle + \langle \delta\hat{I}_{\gamma'}(t') \delta\hat{I}_{\gamma}(t) \rangle \quad (3)$$

in the pseudo-equilibrium state as the expression [1]

$$S_{\gamma\gamma'}(\Omega)\delta(\Omega + \Omega') = \frac{1}{2\pi} \Pi_{\gamma\gamma'}(\Omega, \Omega'), \quad (4)$$

where $\delta\hat{I}_{\gamma}(t) = \hat{I}_{\gamma}(t) - \langle \hat{I}_{\gamma}(t) \rangle$. The symbol $\langle ... \rangle$ in above formula denotes the quantum expectation over the electron state, and the ensemble average over the system. In order to find the shot noise of the system, we have to determine the current correlations between the currents tunneling in the same terminals as well as in different terminals at time t and t'.

The current operator $\hat{I}_\gamma(t)$ for our system is strongly related to the features of terminals. We derive the current operator by considering the continuity equation of electrons, and by employing the Heisenberg equation to give

$$\hat{I}_\gamma(t) = -\frac{ie}{\hbar}\sum_{\delta k\ell\sigma}[\tilde{R}^*_\gamma(t)d^\dagger_{\ell\sigma}(t)c_{\delta\gamma,k\sigma}(t) - \tilde{R}_\gamma(t)c^\dagger_{\delta\gamma,k\sigma}(t)d_{\ell\sigma}(t)]. \quad (5)$$

Due to the coupling and the applied MWF, electrons in the terminals are affected to form nonequilibrium states, and the net current is determined by the transporting electrons from deferent terminals. To determine the current operator, we employ the equation of motion for the electron operators in the leads and QD. The annihilation operator of an electron in the γth terminal is found to be

$$c_{\delta\gamma,k\sigma}(t) = \sum_\ell \int dt_1 g^r_{\delta\gamma,k\sigma}(t,t_1)\tilde{R}_\gamma(t_1)d_{\ell\sigma}(t_1) + \hat{c}_{\delta\gamma,k\sigma}(t), \quad (6)$$

where $\hat{c}_{\delta\gamma,k\sigma}(t)$ is the annihilation operator of electron in the isolated terminal. $g^r_{\delta\gamma,k\sigma}(t,t_1)$ is the Green's function of electron in the isolated γth terminal. This indicates that as there are no interactions between the QD and the terminals, electrons in the terminals satisfy the Fermi distribution function $f(\varepsilon_{\delta\gamma,k\sigma})$ by the form $\langle\hat{c}^\dagger_{\delta\gamma,k\sigma}(t)\hat{c}_{\delta'\gamma',k'\sigma'}(t)\rangle = \delta_{\gamma\gamma'}\delta_{\delta\delta'}\delta_{\sigma\sigma'}\delta_{kk'}f(\varepsilon_{\delta\gamma,k\sigma})$. The operator of electron in the coupled system is involved with the electron operator of the QD, which should also be determined by the equation of motion. Consequently, the annihilation operator of electron in the coupled QD is given by

$$d_{\ell\sigma}(t) = \int dt_1 g^r_{\ell\sigma}(t,t_1)\sum_{\delta\gamma k}\tilde{R}^*_\gamma(t_1)c_{\delta\gamma,k\sigma}(t_1) + \hat{d}_{\ell\sigma}(t), \quad (7)$$

where $\hat{d}_{\ell\sigma}(t)$ is the annihilation operator of electron in the isolated QD, and it has no contribution to the tunneling current. In the following derivations, we drop the operator $\hat{d}_{\ell\sigma}(t)$ for convenient. $g^r_{\ell\sigma}(t,t_1)$ is the corresponding Green's function of the isolated QD. Combining equations (6) and (7), one can obtain the operators of electrons in the terminal and QD by iteration procedure. The annihilation operator of the coupled QD is therefore determined by the coupled Green's function of the QD $G^r_{\ell\sigma}(t,t_1)$ by the expression

$$d_{\ell\sigma}(t) = \int dt_1 G^r_{\ell\sigma}(t,t_1)\sum_{\delta\gamma k}\tilde{R}^*_\gamma(t_1)\hat{c}_{\delta\gamma,k\sigma}(t_1). \quad (8)$$

Substituting the electron operators stated in equations (6)–(8) into the current operator equation (5), we obtain the current operator as

$$\hat{I}_\gamma(t) = \frac{e}{\hbar}\sum_{mn\ell\sigma}\sum_{\beta\beta'}\int\int d\epsilon_1 d\epsilon_2 J_m(\lambda)J_n(\lambda)\Gamma_{\beta\beta'}(\epsilon_1) \times \exp\left(\frac{i}{\hbar}\varepsilon^{nm}_{12}t\right)A^\gamma_{\beta\beta',mn}(\epsilon_1,\epsilon_2)\hat{c}^\dagger_{\beta\sigma}(\epsilon_1)\hat{c}_{\beta'\sigma}(\epsilon_2), \quad (9)$$

where $\varepsilon^{nm}_{ij} = \epsilon_i - \epsilon_j + (n-m)\hbar\omega$, and $J_n(\lambda)$ is Bessel function of the first kind. We have defined the transmission coefficient of the time-dependent system by

$$A^\gamma_{\beta\beta',mn}(\epsilon_1,\epsilon_2) = i\{\delta_{\beta\gamma}G^r_{\ell\sigma}(\epsilon_2+m\hbar\omega) - \delta_{\beta'\gamma}G^a_{\ell\sigma}(\epsilon_1+n\hbar\omega) + [\tilde{\Sigma}^a_{\gamma\sigma}(\epsilon_1+n\hbar\omega) - \tilde{\Sigma}^r_{\gamma\sigma}(\epsilon_2+m\hbar\omega)] \times G^a_{\ell\sigma}(\epsilon_1+n\hbar\omega)G^r_{\ell\sigma}(\epsilon_2+m\hbar\omega)\}.$$

In the above formula, $\Gamma_{\beta\beta'}(\epsilon)$ is the line-width function defined by $\Gamma_{\beta\beta'}(\epsilon) = 2\pi\sum_{\delta k}R_\beta R^*_{\beta'}\delta(\epsilon-\varepsilon_{\delta\beta,k\sigma})$. The line-width function in the same lead is given by $\Gamma_\gamma(\epsilon) = \Gamma_{\gamma\gamma}(\epsilon)$, which reflects the influence of leads on the mesoscopic transport. The line-width function $\Gamma_\gamma(\epsilon)$ of the γth lead defined above is $\Gamma_\gamma(\epsilon) = 2\pi|R_\gamma|^2\rho_\gamma(\epsilon)$. We have introduced the density of state (DOS) of the γth lead $\rho_\gamma(\epsilon) = \sum_{k\delta}\delta(\epsilon-\varepsilon_{\delta\gamma,k\sigma})$, and it can be determined by the Green's function of the lead as $\rho_\gamma(\epsilon) = -\sum_{k\delta}Img^r_{\delta\gamma,k\sigma}(\epsilon)/\pi$. The Fourier transformed Green's function of the γth lead is given by $g^r_{\delta\gamma,k\sigma}(\epsilon) = 1/[\epsilon - \varepsilon_{\delta\gamma,k\sigma} + i\eta]$, $(\eta \to 0)$. The self-energy of the γth lead is given by the modification of MWF to the self-energy in the absence of the field as

$$\tilde{\Sigma}^{r(a)}_{\gamma\sigma}(\epsilon) = \sum_{\delta nk}J^2_n(\lambda)\mid R_\gamma\mid^2 g^{r(a)}_{\delta\gamma,k\sigma}(\epsilon - n\hbar\omega).$$

This self-energy modified by the MWF indicates that the field perturbed line-width function involves side-bands as

$$\widetilde{\Gamma}_\gamma(\epsilon) = 2\pi|R_\gamma|^2\sum_n J^2_n(\lambda)\rho_\gamma(\epsilon - n\hbar\omega).$$

The pseudo-equilibrium retarded (advanced) Green's function of the quantum dot is calculated from solving the Dyson equation. The Fourier transformed version of the Green's function takes the form as

$$G^{r(a)}_{\ell\sigma}(\epsilon) = \frac{1}{\epsilon - \tilde{E}_{\ell\sigma} + eV_g - \tilde{\Sigma}^{r(a)}_\sigma(\epsilon)}, \quad (10)$$

where $\tilde{\Sigma}^{r(a)}_\sigma(\epsilon) = \sum_\gamma\tilde{\Sigma}^{r(a)}_{\gamma\sigma}(\epsilon)$ indicates the total self-energy of the CN terminals.

The time-averaged tunneling current can be observed directly from experiments, and it is found by taking ensemble average and time average over the current operator given in equation (9). The current in the γth CN lead is expressed by

$$I_\gamma = \frac{e}{\hbar}\sum_{m\ell\beta\sigma}\int d\epsilon J^2_m(\lambda)\Gamma_{\beta\beta}(\epsilon)A^r_{\beta\beta,mm}(\epsilon,\epsilon)f_\beta(\epsilon). \quad (11)$$

This is in fact described by the Landauer-Büttiker-like formula

$$I_L = \frac{e}{\hbar}\sum_{mn\ell\sigma}\int d\epsilon T^{LR}_{mn,\ell\sigma}(\epsilon)[f_L(\epsilon - m\hbar\omega) - f_R(\epsilon - n\hbar\omega)], \quad (12)$$

where the quantity $T^{\gamma\beta}_{mn,\ell\sigma}(\epsilon)$ represents the transmission coefficient of electron transporting from the side-band

channel m in one terminal to the side-band channel n in another terminal defined by

$$T^{\gamma\beta}_{mn,\ell\sigma}(\epsilon) = J^2_m(\lambda)J^2_n(\lambda)\Gamma_\gamma(\epsilon - m\hbar\omega) \times\Gamma_\beta(\epsilon - n\hbar\omega)|G^r_{\ell\sigma}(\epsilon)|^2.$$

$G^r_{\ell\sigma}(\epsilon)$ is the retarded Green's function of the coupled QD. The symmetry relation on the transmission coefficient $T^{\gamma\beta}_{mn,\ell\sigma}(\epsilon) = T^{\beta\gamma}_{nm,\ell\sigma}(\epsilon)$ holds in the system. The current is conserved by summing up all of the currents in the terminals, i.e., $\sum_\gamma I_\gamma = 0$. The current formula equation (12) is equivalent to the one derived from the method of Jauho, Wingreen and Meir [29]. We can see obviously that the DOS of a lead plays an important role in the transport. $f_\gamma(\epsilon)$ is the Fermi distribution function defined by $f_\gamma(\epsilon) = 1/\{\exp[(\epsilon - \mu_\gamma)/k_BT] + 1\}$. The spectral density of shot noise is derived by substituting the current operator equation (9) into the correlation function equation (3), and by making Fourier transformation over the two times t and t'. Comparing with the definition of the spectral density of shot noise defined in equation (4), and considering the pseudo-equilibrium state in the presence of the ac field, we find the spectral density of current noise

$$S_{\gamma\gamma'}(\Omega) = \frac{e^2}{h}\sum_{mnn'}\sum_{\ell\ell'}\sum_{\beta\beta'\sigma}\int d\epsilon J_m(\lambda)J_n(\lambda)J_{n'}(\lambda) \times J_p(\lambda)\Gamma_\beta(\epsilon)\Gamma_{\beta'}(\tilde{\epsilon}_{nm})A^\gamma_{\beta\beta',mn}(\epsilon,\tilde{\epsilon}_{nm}) \times A^{\gamma'}_{\beta'\beta,pn'}(\tilde{\epsilon}_{nm},\epsilon)F_{\beta\beta'}(\epsilon,\tilde{\epsilon}_{nm}). \quad (13)$$

We have defined the notations in the above noise formula $\tilde{\epsilon}_{nm} = \epsilon + (n-m)\hbar\omega + \hbar\Omega$, $p = n - m + n'$, and $F_{\beta\beta'}(\epsilon,\tilde{\epsilon}) = f_\beta(\epsilon)[1 - f_{\beta'}(\tilde{\epsilon})] + f_{\beta'}(\tilde{\epsilon})[1 - f_\beta(\epsilon)]$. The effect of photon absorption and emission due to the MWF applied on the QD is included in the noise spectral density. In order to obtain the observed noise spectral density, the absorption and emission of photon numbers are required to satisfy the constraint as $n - m + n' - m' = 0$. In fact, this constriction is the result of energy conservation due to the electron absorbing and emitting photons. This equation indicates the two cases: case (A) for $n = m, n' = m'$, which we refer to the balanced absorption; case (B) for $m' = n - m + n'$, which we refer to the unbalanced absorption.

2.1 Balanced absorption

Substituting the function $A^\gamma_{\beta\beta',mn}$ given in equation (9) into the noise formula (13), we obtain the spectral density of noise for the balanced absorption of the left terminal $S = S_{LL}(0)$ by

$$S = \frac{2e^2}{h}\sum_{mn}\sum_{\ell\ell'\sigma}\int d\epsilon J^2_m(\lambda)J^2_n(\lambda)\Big\{\sum_{\beta\neq\beta'}\Gamma^2_\beta(\epsilon)\widetilde{\Gamma}_{\beta'}(\epsilon + n\hbar\omega) \times\widetilde{\Gamma}_{\beta'}(\epsilon + m\hbar\omega)\, f_\beta(\epsilon)[1 - f_\beta(\epsilon)] + \Gamma_L(\epsilon)\Gamma_R(\epsilon)Y^{nm}_{\ell\ell'}(\epsilon)F_{LR}(\epsilon)\Big\} \times |\, G^r_{\ell\sigma}(\epsilon + n\hbar\omega)\,|^2 |\, G^r_{\ell'\sigma}(\epsilon + m\hbar\omega)\,|^2\,. \quad (14)$$

We have defined the notations $Y^{np}_{\ell\ell'}(\epsilon) = \widetilde{\Gamma}_L(\epsilon + n\hbar\omega)\widetilde{\Gamma}_R(\epsilon + p\hbar\omega)\{X_{\ell\ell'}(\epsilon + n\hbar\omega, \epsilon + p\hbar\omega) - 1\}$ in which the function $X_{\ell\ell'}(\epsilon_1,\epsilon_2)$ is expressed as

$$X_{\ell\ell'}(\epsilon_1,\epsilon_2) = \frac{\widetilde{\Gamma}(\epsilon_1)\widetilde{\Gamma}(\epsilon_2)/4 + w_{\ell\sigma}(\epsilon_1)w_{\ell'\sigma}(\epsilon_2)}{\widetilde{\Gamma}_L(\epsilon_1)\widetilde{\Gamma}_R(\epsilon_2)},$$

where $w_{\ell\sigma}(\epsilon) = \epsilon - \tilde{E}_{\ell\sigma} + eV_g - \mathrm{Re}\tilde{\Sigma}^r_\sigma(\epsilon)$, and $\widetilde{\Gamma}(\epsilon) = \sum_\gamma \widetilde{\Gamma}_\gamma(\epsilon)$. The formula contains thermal noise and shot noise. We can see that the thermal noise for this case is explicitly expressed by the first term which contains the function $f_\beta(\epsilon)[1 - f_\beta(\epsilon)]$. The thermal noise disappears as the temperature approaches zero. At zero temperature, the shot noise of the balanced absorption case is zero as the source-drain bias V is removed. This indicates that the photon-electron pumped currents from QD to the terminals are equal, and the self-correlation of currents is zero due to the symmetric pumping. The source-drain bias disturbs the balance of symmetric pumping, and the self-correlation of currents is nonzero in the presence of the biased voltage V.

2.2 Unbalanced absorption

The unbalanced absorption situation is quite different from the balanced one. The noise spectral density of the left terminal $S = S_{LL}(0)$ is derived from equation (13) as

$$S = \frac{2e^2}{h}\sum_{mnn'}\sum_{\ell\ell'\sigma}\int d\epsilon J_m(\lambda)J_n(\lambda)J_{n'}(\lambda)J_p(\lambda) \times\Big\{\frac{1}{2}\sum_{\beta\neq\beta'}\Gamma_\beta(\epsilon)\Gamma_\beta(\tilde{\epsilon}_{nm})\widetilde{\Gamma}_{\beta'}(\epsilon + n\hbar\omega)\widetilde{\Gamma}_{\beta'}(\epsilon + p\hbar\omega) \times F_{\beta\beta}(\epsilon,\tilde{\epsilon}_{nm}) + \Gamma_L(\epsilon)\Gamma_R(\tilde{\epsilon}_{nm})Y^{np}_{\ell\ell'}(\epsilon)F_{LR}(\epsilon,\tilde{\epsilon}_{nm})\Big\} \times|G^r_{\ell\sigma}(\epsilon + n\hbar\omega)\,|^2\,|G^r_{\ell'\sigma}(\epsilon + p\hbar\omega)\,|^2, \quad (15)$$

where $p = n - m + n'$. From the formula we can observe that the first term of the noise spectral density contains thermal noise and shot noise. This means that the thermal noise term corresponding to the balanced case shown in equation (14) is perturbed by the applied ac field, and it is nonzero even if the temperature approaches zero. So that this term also contains shot noise induced by the ac field. As temperature approaches zero, the excess noise of this term make contribution to the total shot noise. The second term represents the shot noise induced both by the source-drain bias and the applied ac field. This signifies that the self-correlation of current is nonzero if the source-drain bias or the ac field is present.

3 Numerical calculations

Although the derivations of the shot noise in the above section are related to the more general situation for the

multi-level QD system, in the numerical calculations we consider the special situation of single-level QD $\tilde{E}_{0\sigma} = 0$ system. Generally, the Coulomb interaction exists in the electron system, and the interaction becomes stronger as the sample becomes smaller. However, we can restrict our investigation to consider the tunneling in the neighborhood of a single Coulomb oscillation peak [34,35]. The theoretical consideration on this restriction can be described by a single channel QD model approximately. The experimental observation for the physics around this level can be achieved by detecting the tunneling behaviors and noise near this energy region. From the investigation, one can grasp the main behaviors of shot noise in the CN-QD-CN system irradiated with MWF. According to the weakly coupled system between the two leads and QD, the coupling strengthes are chosen as the symmetric parameters $R_L = R_R = 24.5$ or 17.5 meV. We also perform the numerical calculations for the system composed of normal metal terminals for comparison. For such system, we choose the DOS of metal terminals by $\rho_L = 0.165/eV$, which corresponds to the line-width of a metal lead as $\Gamma_L = 1.24$ meV. We consider the external microwave field located in the frequency region 10^{11} Hz with the photon energy $\hbar\omega = 2.0$ meV (corresponding to the frequency 4.78×10^{11} Hz). We perform the numerical calculations to show the shot noise versus source-drain bias, gate voltage, and frequency. The Fano factor and differential shot noise are also calculated for the balanced and unbalanced absorptions. Since we are interested in the shot noise under the perturbation of MWF, we deal with the zero-temperature circumstance, where the thermal noise becomes zero. We take γ_0 as the energy scale for the energy quantities in the calculations. The CN leads are chosen as the armchair (9, 9) CN, whose DOS structure can be found in reference [15]. The differential shot noise dS/dV is scaled by $2e^3/h$, and the shot noise is scaled by $S_0 = 2e^2\gamma_0/h$.

3.1 Balanced absorption

In this subsection, we perform the numerical calculations of shot noise and Fano factor for the balanced absorption by employing equation (14).

We display the differential shot noise dS/dV of CN-QD-CN system versus the source-drain bias eV in Figure 1 as $V_g = 0$. Diagrams (a) and (b) are associated with the systems in the absence and presence of MWF with the parameter $\Lambda = 0$ and $\Lambda = 0.8$ correspondingly. As the source-drain bias eV is positive, dS/dV shows positively resonant structure, while it displays negatively reverse resonant behavior as eV is negative. This is the reflection of asymmetric behavior as $dS(eV)/dV = -dS(-eV)/dV$. For the QD coupled to two metal leads and in the absence of MWF, there exists only one positive peak as $eV > 0$, and a negatively inverse resonant peak as $eV < 0$. The splitting of resonant peaks is induced by the coupled carbon nanotubes. This is resulted from the fact that the CNs provide multi-channels for electrons to transport through. The DOS of a CN lead contributes to the real part of

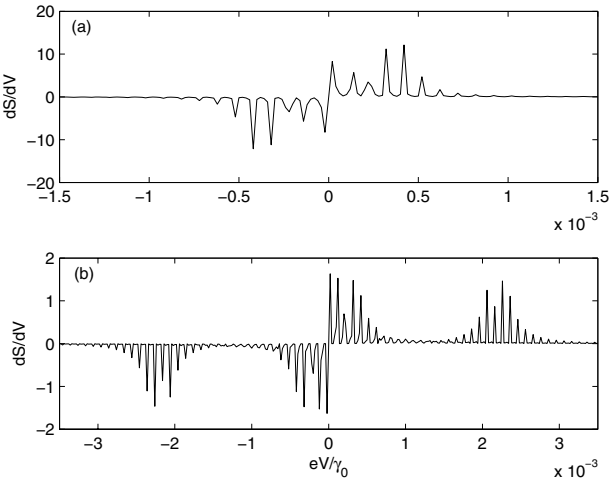

Fig. 1. The differential shot noise dS/dV of CN-QD-CN system versus source-drain bias eV for the balanced case. The parameters are chosen as $eV_g = 0$, $R_\gamma = 24.5$ meV, $\hbar\omega = 2.0$ meV, and $\Lambda = 0$ for diagram (a); $\Lambda = 0.8$ for diagram (b).

self-energy of the terminal, and this causes the splitting of energy level in the QD. As the external MWF is applied to the QD, novel side-bands of QD emerge for electrons to tunnel, which result in the photon-assisted tunneling (PAT). The PAT effect is obviously exhibited in diagram (b) by splitting and adding new resonant peaks compared with diagram (a).

The shot noise spectral density and Fano factor versus gate voltage are depicted in Figure 2 as $eV = 1.5165$ meV, and $\hbar\omega = 2.0$ meV. Diagram (a) represents the shot noise with different coupling strengths R_γ. We find the shot noise is intimately related to the couplings. As the coupling is weaker as $R_\gamma = 10.0$ meV, single resonant peak dominates the shot noise. While as $R_\gamma = 17.5$ meV, the single-peak structure is competed by the splitting effect of the system, and two side peaks emerge on the shoulders compared with the situation possessing smaller R_γ. The appearing of side peaks results from the DOS of CNs and the competition of the coupling strengths. As the coupling strengths become large enough, say $R_\gamma = 24.5$ meV, the interaction strengths enhance the splitting effect, and double resonant structure exhibits. Diagram (b) displays the shot noise in the absence ($\Lambda = 0$), and in the presence ($\Lambda = 0.8$) of external microwave field. The shot noise is affected by the MWF in both of the magnitude and form. In the absence of MWF, the magnitude of the shot noise is about 0.9×10^{-4} S_0. The MWF suppresses it to the value of 0.4×10^{-4} S_0. Novel steps emerge on the sides of the resonant peak of shot noise when MWF is applied. The Fano factor is added in diagram (c) to exhibit the deviation of shot noise and corresponding current versus gate voltage. Inverse resonant behavior is observed in the Fano factor, and the side-steps emerge as the MWF is applied to the QD. In the regime approximate to $|eV_g| < 2 \times 10^{-3}$ γ_0, the MWF contributes more suppression effect to shot noise than that of the situation in the absence of MWF. The Fano factors for the two cases become the same as $|eV_g| \gg 2 \times 10^{-3}$ γ_0, which is the saturated value of Fano factor $F = 0.125$.

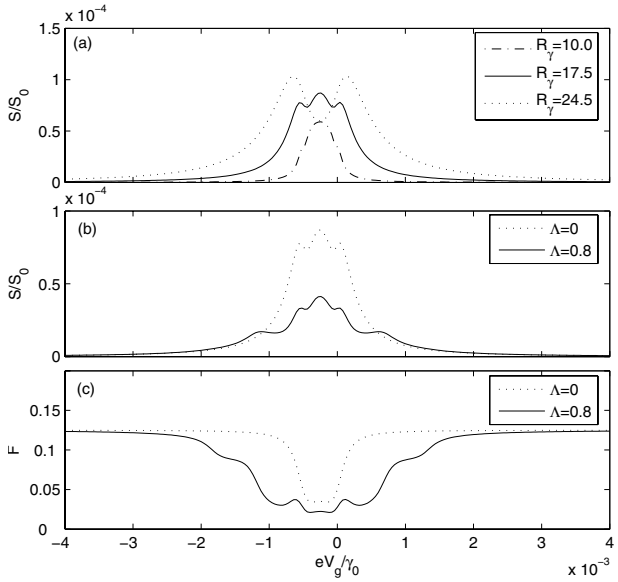

Fig. 2. The shot noise and Fano factor versus gate voltage for the balanced case. The parameters are chosen as $eV = 1.5165$ meV, and $\hbar\omega = 2.0$ meV. Diagram (a) shows the variation of shot noise associated with different coupling strengths as $R_\gamma = 10.0, 17.5, 24.5$ meV, respectively as $\Lambda = 0$. Diagram (b) displays the shot noise versus gate voltage when $\Lambda = 0$ and 0.8, respectively. Diagram (c) is the Fano factor versus gate voltage when $\Lambda = 0$ and 0.8, respectively.

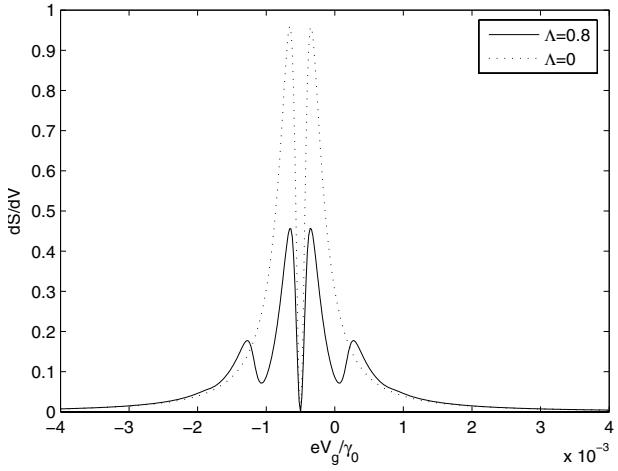

Fig. 3. The differential shot noise dS/dV versus gate voltage for the balanced case as $R_\gamma = 17.5$ meV and $eV = 1.5165$ meV. The dotted curve is related to the system in the absence of MWF, while the solid curve is associated with the system applied with MWF of frequency $\hbar\omega = 2.0$ meV as $\Lambda = 0.8$.

The differential shot noise dS/dV versus gate voltage V_g is exhibited in Figure 3 as source-drain bias $eV = 1.5165$ meV. The dotted curve represents the situation in the absence of MWF. Double resonant peaks appear with the heights about $0.98 \times 2e^3/h$. The double resonant peaks signify the splitting of single resonant transport peak of transmission in the QD coupled system. This can be understood from the formula as $dS/dV \sim T(\epsilon)[1 - T(\epsilon)]$ for a single-level system. As the transmission coefficient

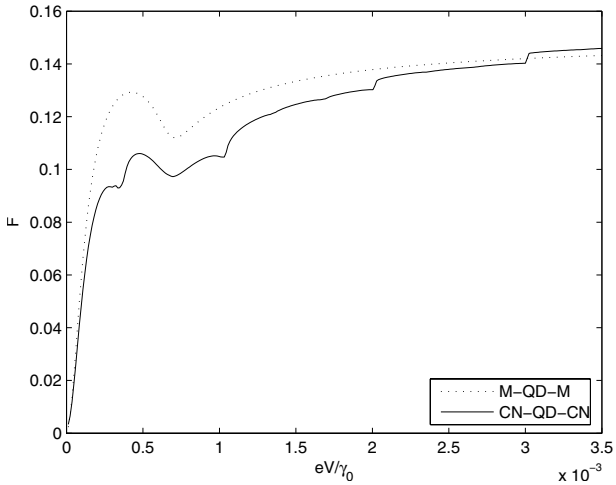

Fig. 4. The Fano factor versus source-drain bias eV for the balanced case. The parameters are chosen as $\hbar\omega = 2.0$ meV, $eV_g = 0, R_\gamma = 17.5$ meV, and $\Lambda = 0.8$.

approaches its resonant value 1, $dS/dV \to 0$. The perturbation of external MWF induces two novel side peaks, which are associated with the PAT procedure of absorption and emission photons when electrons tunnel through the system. The applied MWF suppresses the magnitude of dS/dV to the value $0.48 \times 2e^3/h$, and the suppression causes the emergence of side-peaks as compensation.

Figure 4 displays the Fano factor in the presence of MWF varying with the source-drain bias. The solid curve indicates the situation of CN-QD-CN, while the dotted curve is for the system of a QD coupled to the normal metal leads. The Fano factor increases from zero with increasing the biased voltage V. As the source-drain bias increases to the value $eV \approx 0.45 \times 10^{-3}\ \gamma_0$, an obvious peak appears, and then the Fano factor declines to form a valley for the M-QD-M system. The Fano factor contains step-like behavior, which is intimately related to the structure of CNs. As the biased voltage is small, there exists distinct difference between the Fano factors of the two systems. However, as the voltage is large, $eV \gg 3.5 \times 10^{-3}\ \gamma_0$, the same saturated value $F \approx 0.142$ is realized for both of the two systems. The Fano factor for the balanced system is smaller than 1 in the whole regime of eV, which indicates that the shot noise of the balanced system belongs to the sub-Poissonian.

We present corresponding behaviors of shot noise, tunneling current, and Fano factor versus the photon energy in Figure 5. The shot noise varies non-monotonically in the small regime of photon energy, and a valley appears at about $\hbar\omega = 0.45 \times 10^{-3}\ \gamma_0$ shown in Diagram (a). Then it increases to its saturated value $S = 0.75 \times 10^{-4}\ S_0$ as the photon energy $\hbar\omega \gg 1.5 \times 10^{-3}\ \gamma_0$. The corresponding current versus photon energy is depicted in diagram (b) for comparing with the shot noise. One observes that there exists distinct differences between the shot noise and current. This difference is evidently given by the Fano factor shown in diagram (c). The Fano factor varies drastically as the photon energy is small, and also a valley is observed near $\hbar\omega = 0.45 \times 10^{-3}\ \gamma_0$. It then increases from

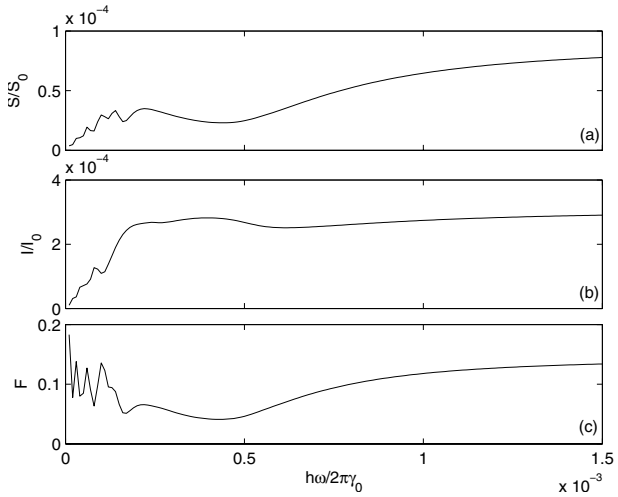

Fig. 5. The shot noise, current, and Fano factor versus photon energy $\hbar\omega$ for the balanced case. The parameters are chosen as $eV = 1.5165$ meV, $eV_g = 0$, $R_\gamma = 24.5$ meV, and $eV_d = 1.6$ meV.

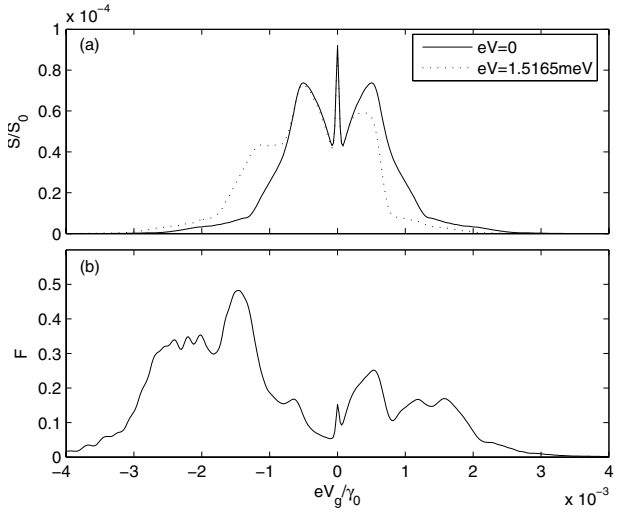

Fig. 6. The shot noise S and Fano factor F versus gate bias eV_g for the unbalanced case. The parameters are chosen as $\Lambda = 0.8$, $\hbar\omega = 2.0$ meV, and $R_\gamma = 17.5$ meV for both of (a) and (b); while for (b) $eV = 1.5165$ meV.

the valley to its saturated value $F \approx 0.145$. The behavior of Fano factor versus photon energy is different from the one varying with respect to source-drain bias shown in Figure 4.

3.2 Unbalanced absorption

We perform the numerical calculations of shot noise and Fano factor for the unbalanced absorption in this subsection by employing equation (15).

We display the shot noise and Fano factor versus gate voltage in Figure 6. Diagram (a) is the shot noise associated with the case as $eV = 0$ (solid curve), and $eV = 1.5165$ meV (dotted curve), correspondingly. The

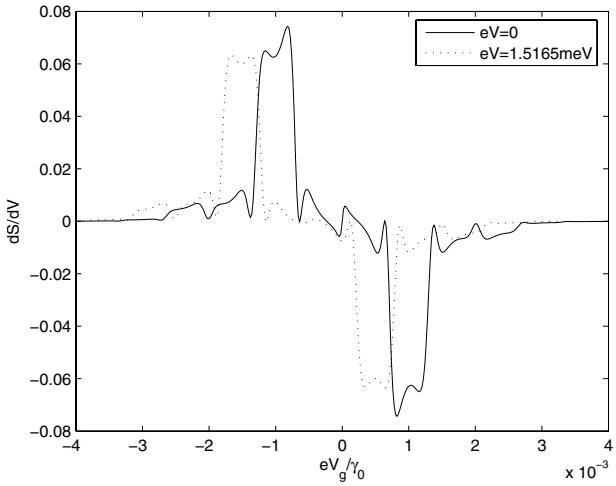

Fig. 7. The differential shot noise dS/dV versus gate bias eV_g for the unbalanced case. The parameters are chosen as $\Lambda = 0.8$ and $R_\gamma = 17.5$ meV, and $eV = 1.5165$ meV.

shot noise for the unbalanced situation is nonzero as the source-drain bias is removed, even if the corresponding current is zero for the symmetric circumstance. For our symmetric system where the two leads and the coupling strengths are assumed to be equal, the MWF pumps equal electrons from the QD to the two leads. As a result, the pumped electrons do not form net current in the absence of source-drain bias. However, the pumped electrons may produce shot noise, which is photon-assisted effect induced by the MWF. This effect is quite different from the case of balanced absorption. As the source-drain bias switches on, the shot noise exhibits asymmetric behavior shown by the dotted curve. This behavior indicates that the unbalanced absorption of photons and biased voltage together destroy the symmetric structure compared with Figure 2 for the balanced case. This asymmetry property is transferred to the Fano factor shown in diagram (b), and the Fano factor is larger than the one in the case of balanced absorption.

The asymmetric behavior is even more distinctly shown by the differential shot noise depicted in Figure 7. Positive and negative values display in dS/dV versus gate voltage. Compared with the balanced case shown in Figure 2, one recognizes that the balanced and unbalanced absorption procedures induce completely different effects. The positive and negative behaviors are the results of the competition for absorbing photons. From the noise formula given by equation (15), the shot noise is sensitive to the source-drain bias. However, as $eV = 0$, the photon energy provides the role of source-drain bias. This bias varies with the integers of absorption and emission of photons. Therefore, the positive and negative behaviors of dS/dV are arisen.

Figure 8 shows the shot noise S and Fano factor F versus photon energy. Several resonant peaks arise in the shot noise as the photon energy $\hbar\omega$ is small, and the shot noise increases to the height $10^{-4}\ S_0$ at about $\hbar\omega = 0.3 \times 10^{-3}\ \gamma_0$. The saturated value $1.2 \times 10^{-4}\ S_0$ of shot noise reaches as $\hbar\omega \gg 10^{-3}\ \gamma_0$. Compared with the

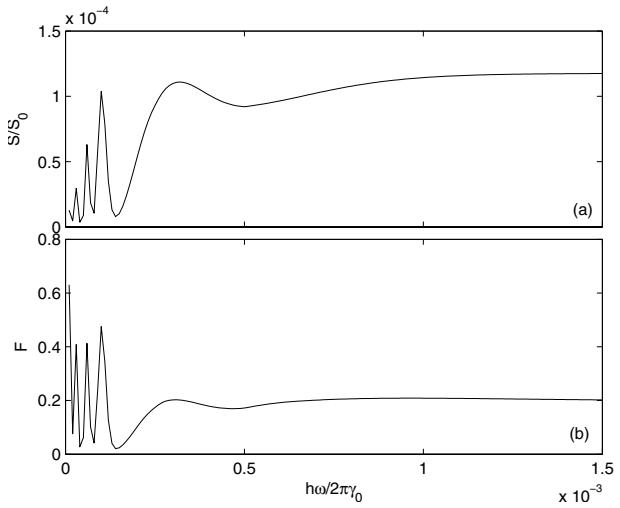

Fig. 8. The shot noise and Fano factor versus photon energy $\hbar\omega$ for the unbalanced case. The parameters are chosen as $eV = 1.5165$ meV, $R_\gamma = 24.5$ meV, $eV_d = 1.6$ meV, and $eV_g = 0$.

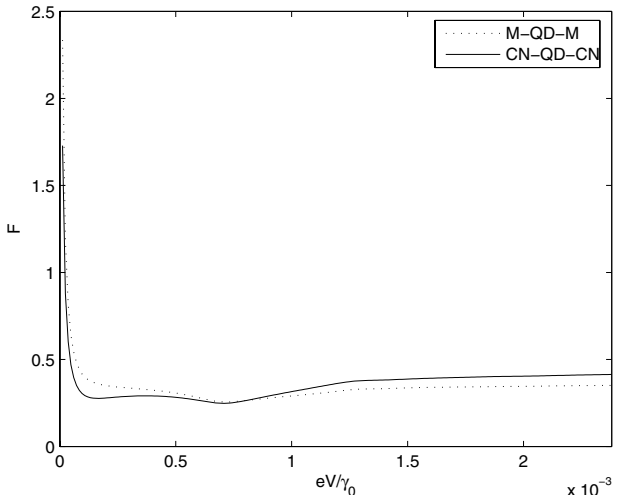

Fig. 9. The Fano factor versus source-drain bias eV for the unbalanced case. The parameters are chosen as $R_\gamma = 17.5$ meV, $eV_g = 0$, $\hbar\omega = 2.0$ meV, and $\Lambda = 0.8$.

shot noise for the balanced case shown in Figure 5, we see that the shot noise of the unbalanced case is larger than that of the balanced one. This is because that for the unbalanced absorption, the thermal term becomes nonequilibrium noise, while the one in the balanced case is still an equilibrium noise even in the presence of MWF. The Fano factor also resonates drastically as the photon energy is small, and it reaches the saturated value about $F = 0.2$. The behavior of the Fano factor tells us that the shot noise and current behave quite differently as the photon energy is small.

The Fano factor versus source-drain bias eV is presented in Figure 9 to show the behavior related to the enhancement and suppression of shot noise. One observes that as the source-drain bias is small enough, the Fano factor becomes greater than one, $F > 1$. As the bias eV increases to a definite value, the Fano factor is lesser than one, $F < 1$. This situation implies that the shot noise is not always sub-Poissonian, it may be super-Poissonian by changing the source-drain bias. Since as $eV = 0$, the tunneling current is zero due to the symmetric photon-electron pumping. However, the shot noise is induced by the photon-electron pumping. From the formula of shot noise equation (15), one recognizes that the contribution of shot noise comes from both of the photon perturbed thermal noise and transporting noise as $eV \to 0$, and $T \to 0$. Compared with the Fano factors between the balanced and unbalanced absorptions, we obtain that the shot noises of the two cases belong to different types. The shot noise for the unbalanced absorption possesses larger saturated Fano factor than that of the balanced situation, which also indicates the enhancement of shot noise due to the unbalanced absorption of photons.

4 Summary and discussion

We have investigated the spectral density of shot noise for the system of CN-QD-CN irradiated with a MWF on the QD. The noise is derived from the equation of motion method incorporated with the nonequilibrium Green's function of QD. The terminal features are involved in the shot noise through modifying the self-energy of QD. The DOS of CN leads contribute to the noise both on the energy-splitting and the line-width of resonances. The MWF provides side-bands for electron to tunnel, and the irradiation of MWF induces compound effect of photon absorption and emission. This arises the balanced absorption and unbalanced absorption procedures related to the shot noise, and they behave quite differently in our system. The contributions of CN leads to the shot noise exhibit obvious behaviors when the biased voltage and energies are closed to the energy level of QD.

For the balanced absorption, the shot noise spectral density and the differential shot noise appear symmetric resonant structures. The external MWF contributes the effect of adding photon resonant side peaks to form shoulders of shot noise and differential shot noise. The novel side peaks are associated with the PAT procedure of absorption and emission of photons accompanying the suppression of shot noise. The Fano factor of balanced system is always smaller than one, which indicates that the shot noise in this case belongs to sub-Poissonian. The shot noise of the unbalanced situation is nonzero as the source-drain bias is removed, even if the corresponding current is zero for the symmetric circumstance. The shot noise exhibits asymmetric behavior, which implies that the unbalanced absorption of photons and biased voltage together destroy the symmetry of shot noise and differential shot noise. The shot noise of the unbalanced case is larger than that of the balanced one. The Fano factor resonates drastically as the photon energy is small, which tells us that the shot noise and current behave quite differently. The shot noise is not always sub-Poissonian, it may be super-Poissonian by changing the source-drain bias for the unbalanced absorption.

This work was supported by the National Natural Science Foundation of China under the Grant No. 10375007, and by the Fundamental Research Foundation of Beijing Institute of Technology.

References

1. M. Büttiker, Phys. Rev. Lett. **68**, 843 (1992); M. Büttiker, Phys. Rev. B **46**, 12485 (1992); Ya.M. Blanter, M. Büttiker, Phys. Rep. **336**, 1 (2000)
2. Y. Imry, *Introduction to Mesoscopic Physics* (Oxford University Press, New York, Oxford, 1997)
3. W. Schottky, Ann. Phys. (Leipzig) **57**, 541 (1918)
4. M.J.M. de Jong, C.W.J. Beenakker, Phys. Rev. B **46**, 13400 (1992); M.J.M. de Jong, C.W.J. Beenakker, Phys. Rev. B **49**, 16070 (1994)
5. H.K. Zhao, Phys. Lett. A **299**, 262 (2002); H.K. Zhao, Int. J. Mod. Phys. B **16**, 3503 (2002)
6. Y.P. Li, D.C. Tsui, J.J. Heremans, J.A. Simmons, G.W. Weimann, Appl. Phys. Lett. **57**, 774 (1990)
7. M. Reznikov, M. Heiblum, H. Shtrikman, D. Mahalu, Phys. Rev. Lett. **75**, 3340 (1995)
8. A. Kumar, L. Saminadayar, D.C. Glattli, Y. Jin, B. Etienne, Phys. Rev. Lett. **76**, 2778 (1996)
9. V.V. Kuznetsov, E.E. Mendez, X. Zuo, G.L. Snider, E.T. Croke, Phys. Rev. Lett. **85**, 397 (2000)
10. A.N. Korotkov, K.K. Likharev, Phys. Rev. B **61**, 15975 (2000)
11. O.M. Bulashenko, J.M. Rubí, Phys. Rev. B **64**, 045307 (2001); O.M. Bulashenko, J.M. Rubí, Phys. Rev. B **67**, 115322 (2003)
12. G. Iannaccone, G. Lombardi, M. Macucci, B. Pellegrini, Phys. Rev. Lett. **80**, 1054 (1998)
13. S.S. Safonov et al., Phys. Rev. Lett. **91**, 136801 (2003)
14. S. Iijima, Nature (London) **354**, 56 (1991)
15. R. Saito, G. Dresselhaus, M.S. Dresselhaus, *Physical Properties of Carbon Nanotubes* (Imperial College Press, London, 1998)
16. Z. Yao, H.W.Ch. Postma, L. Balents, C. Dekker, Nature (London) **402**, 273 (1999)
17. A.A. Odintsov, Phys. Rev. Lett. **85**, 150 (2000)
18. S.J. Tans, A.R.M. Verschueren, C. Dekker, Nature (London) **393**, 49 (1998)
19. D. Loss, D.P. Divincenzo, Phys. Rev. A **57**, 120 (1998)
20. W. Tian, S. Datta, Phys. Rev. B **49**, 5097 (1994); Y. Xue, S. Datta, Phys. Rev. Lett. **83**, 4844 (1999)
21. H. Mehrez, J. Taylor, H. Guo, J. Wang, C. Roland, Phys. Rev. Lett. **84**, 2682 (2000); C. Roland, M.B. Nardelli, J. Wang, H. Guo, Phys. Rev. Lett. **84**, 2921 (2000)
22. J. Kong, E. Yenilmez, T.W. Tombler, W. Kim, H. Dai, Phys. Rev. Lett. **87**, 106801 (2001)
23. S.J. Tans, M.H. Devoret, H. Dai, A. Thess, R.E. Smalley, L.J. Geerligs, C. Dekker, Nature (London) **386**, 474 (1997)
24. F. Léonard, J. Tersoff, Phys. Rev. Lett. **83**, 5174 (1999)
25. H.K. Zhao, Phys. Lett. A **308**, 226 (2003); H.K. Zhao, Phys. Lett. A **310**, 207 (2003); H.K. Zhao, Eur. Phys. J. B **33**, 365 (2003)
26. H. Mehrez, H. Guo, J. Wang, C. Roland, Phys. Rev. B **63**, 245410 (2001)
27. T.H. Oosterkamp, T. Fujisawa, W.G. van der Wiel, K. Ishibashi, R.V. Hijman, S. Tarucha, L.P. Kouwenhoven, Nature (London) **395**, 873 (1998)
28. Q.F. Sun, J. Wang, T.H. Lin, Phys. Rev. B **61**, 12643 (2000)
29. A.P. Jauho, N.S. Wingreen, Y. Meir, Phys. Rev. B **50**, 5528 (1994)
30. L.N. Zhao, H.K. Zhao, Int. J. Mod. Phys. B **18**, 2071 (2004); L.N. Zhao, H.K. Zhao, Eur. Phys. J. B **42**, 285 (2004); L.N. Zhao, H.K. Zhao, Phys. Lett. A **325**, 156 (2004)
31. H.K. Zhao, J. Wang, Phys. Lett. A **323**, 285 (2004); H.K. Zhao, J. Wang, Eur. Phys. J. B **40**, 93 (2004)
32. H.K. Zhao, L.N. Zhao, Eur. Phys. J. B **47**, 295 (2005); H.K. Zhao, J. Wang, Q. Wang, Eur. Phys. J. B **51**, 425 (2006)
33. M.H. Pedersen, M. Büttiker, Phys. Rev. B **58**, 12993 (1998)
34. Q.F. Sun, J. Wang, T.H. Lin, Phys. Rev. B **61**, 13032 (2000)
35. A.P. Jauho, N.S. Wingreen, Phys. Rev. B **58**, 9619 (1998)